Electrochromic Shift of Chlorophyll Absorption in Photosystem I from *Synechocystis* sp. PCC 6803: A Probe of Optical and Dielectric Properties around the Secondary Electron Acceptor

Naranbaatar Dashdorj,* Wu Xu,† Peter Martinsson,‡ Parag R. Chitnis,† and Sergei Savikhin*
*Department of Physics, Purdue University, West Lafayette, Indiana 47907; †Department of Biochemistry, Biophysics, and Molecular Biology, and ‡Department of Chemistry, Iowa State University, Ames, Iowa 50011

ABSTRACT Nanosecond absorption dynamics at ~685 nm after excitation of photosystem I (PS I) from *Synechocystis* sp. PCC 6803 is consistent with electrochromic shift of absorption bands of the Chl *a* pigments in the vicinity of the secondary electron acceptor A_1. Based on experimental optical data and structure-based simulations, the effective local dielectric constant has been estimated to be between 3 and 20, which suggests that electron transfer in PS I is accompanied by considerable protein relaxation. Similar effective dielectric constant values have been previously observed for the bacterial photosynthetic reaction center and indicate that protein reorganization leading to effective charge screening may be a necessary structural property of proteins that facilitate the charge transfer function. The data presented here also argue against attributing redmost absorption in PS I to closely spaced antenna chlorophylls (Chls) A38 and A39, and suggest that optical transitions of these Chls, along with that of connecting chlorophyll (A40) lie in the range 680–695 nm.

INTRODUCTION

Electrostatic forces play a crucial role in the conformation and function of biomolecules, especially in the protein complexes that carry out charge transfer functions. Due to the presence of a mixture of neutral, polar, and charged chains in proteins, the charge transfer processes involve complex reorganization of the local protein environment, leading to effective charge screening (Treutlein et al., 1992; Steffen et al., 1994; Simonson and Brooks, 1996). This local reorganization, along with the redox potential difference between electron donor and acceptor, is a key factor in defining the efficiency of electron transfer (Moser et al., 1992). The fundamental constant defining the strength of electrostatic screening is the relative static dielectric permittivity (dielectric constant) ε_r. Numerous model calculations predict that a typical average dielectric permittivity for protein in water ranges from 10 to 80 (King et al., 1991; Smith et al., 1993; Simonson and Brooks, 1996; Löffler et al., 1997; Simonson, 1998; Pitera et al., 2001). Major contributors to this value are relatively flexible polar side chains on the outer surface of the protein. The dielectric constant deep within the protein is expected to drop to 2–4, which agrees with the known low polarizability of dry powders where the absence of water restricts the mobility of the peripheral side chains (Rosen, 1963; Bone and Pething, 1982, 1985). Despite considerable interest, the number of direct measurements of protein dielectric constant and charge screening is relatively small, as such measurements present an experimental challenge. Standard experimental approaches to the problem include measurements of pK_a and redox potential shifts due to point mutations (Russell and Fersht, 1987; Varadarajan et al., 1989), and measurements of gas-phase basicities of protein ions (Schnier et al., 1995). Protein function relies on its rich microscopic structure, which implies that the effective (local) dielectric constant varies within the bulk of a protein. These variations in the local dielectric environment may play a decisive role in electron transfer systems, and can be observed by measuring electrochromic shifts of spectroscopic probes embedded into the protein structure (Lockhart and Kim, 1992; Pierce and Boxer, 1992; Steffen et al., 1994). In this article, we report on measurements of the effective (local) dielectric constant in photosystem I in the vicinity of the secondary electron acceptor A_1, by observing the electrochromic shift of the nearest chlorophyll absorption bands in response to electron transfer from the secondary electron acceptor A_1.

Photosystem I (PS I) is a chlorophyll-protein complex that uses light energy to reduce ferredoxin in cyanobacteria and higher green plants (Brettel, 1997). The discovery and subsequent refinements of the x-ray crystal structure of the PS I core antenna-reaction center complex from the cyanobacterium *Synechococcus elongatus* (Krauss et al., 1993, 1996; Klukas et al., 1999; Jordan et al., 2001) have stimulated great interest in its structure-function relationships. The PS I reaction center contains six chlorophyll (Chl) *a* cofactors: the P700 special pair Chls (analogous to the special pair bacteriochlorophylls in purple bacterial reaction centers), two accessory Chls (analogous to the accessory bacteriochlorophylls), and two chlorophylloid primary electron acceptors A_0. In the PS I reaction center, primary charge separation leads to the reduction of A_0, creating the radical ion pair $P700^+A_0^-$. The unpaired electron migrates first to the phylloquinone secondary acceptor A_1, then to the 4Fe-4S center F_X, and finally to the terminal iron-sulfur

Submitted June 12, 2003, and accepted for publication December 23, 2003.

Address reprint requests to Sergei Savikhin, E-mail: sergei@physics.purdue.edu.

Wu Xu's present address is Dept. of Biochemistry, St. Jude Children's Research Hospital, Memphis, TN 38105.

0006-3495/04/05/3121/10 $2.00

electron acceptors F_A and F_B before being harvested by ferredoxin (Brettel, 1997).

The kinetics of the primary events are well known for the purple bacterial reaction center (Zinth and Kaiser, 1993; Woodbury and Allen, 1995). The primary charge separation $PH \rightarrow P^+H^-$ requires 2–3 ps at room temperature, and the subsequent electron transfer to the primary quinone Q_A (which is analogous to A_1 in PS I) exhibits multiphasic kinetics (80–300 ps). The scenario is less clear for PS I. It is widely believed (Brettel, 1997) that the creation of the radical pair $P700^+A_0^-$ occurs within 1–3 ps after the creation of the electronically excited special pair P700*. Most estimates of the timescale for the $A_0^- \rightarrow A_1$ electron transfer in wild-type PS I range from 10 to 50 ps (Hastings et al., 1994; Brettel and Vos, 1999; Iwaki et al., 1995; Kumazaki et al., 1994; White et al., 1996; Savikhin et al., 2001), whereas the $A_1^- \rightarrow F_X$ electron transfer occurs with dual ~10 ns and 200–280 ns kinetics (Bock et al., 1989; van der Est et al., 1994; Brettel, 1988, 1998; Setif and Brettel, 1993; Sakuragi et al., 2002). Hence, there is general agreement that in PS I the reduction of A_1 is complete within a few tens of picoseconds at most and the Chl Q_y spectral evolution that stems from the preceding primary processes are essentially complete within this time. Although the consequent electron transfer from A_1^- to the iron sulfur complexes do not affect the Chl population directly, the presence of a strong local electric field around these electron transfer cofactors must affect the optical properties of the nearby pigments (Steffen et al., 1994). Recently, Savikhin et al. (2001) reported that noticeable optical absorption evolution in the Chl Q_y spectral region spans well into the nanosecond range, and suggested protein relaxation as a possible cause of the observed signal. In this article, we have performed detailed analysis of this effect and propose that the shape and magnitude of these changes are more consistent with an electrochromic shift of the Chl absorption bands that accompanies electron transfer from A_1 to F_X. Based on the measured data, we are able to estimate the effective dielectric constant deep within PS I. Considerable local reorganization of the interior of the protein must also occur, leading to effective charge screening. These results are consistent with similar measurements of the effective dielectric constant within the bacterial reaction center (Steffen et al., 1994).

EXPERIMENTAL METHOD

Excitation pulses (660 nm, ~100 fs full width at half-maximum) were generated using a self-mode-locked Ti:sapphire laser, regenerative amplifier, optical parametric amplifier, and frequency doubler as described earlier (Savikhin et al., 2000). Probe pulses (675–702 nm, 10–15 ns full width at half-maximum) originated in a cavity-dumped dye laser (DCM laser dye) tuned with an intracavity birefringent filter. The cavity dumper timing was derived from sync output pulses of the Pockels cell driver in the pump laser's regenerative amplifier. Variable delays were generated in a modified EG&G (Gaithersburg, MD) GD150 delay line, with its external delay input connected to a PC digital-to-analog converter output. After conversion to 10-ns-long TTL pulses using a Tektronix PG501 pulse generator (Beaverton, OR), the GD150 output pulses were directed to the dye laser cavity dumper. The resulting delay precision was observed to be better than 1 ns. Sample transmission of the probe pulses was determined using home-built photodiode detectors combined with a boxcar integrator (Savikhin et al., 2000). The transient spectrum at 200 ps after excitation was probed using femtosecond continuum pulses (Savikhin et al., 2000). $P700^+$-P700 spectral differences 3 s after excitation were measured by a modified Perkin-Elmer (Wellesley, MA) absorption spectrometer (Savikhin et al., 2000).

Trimeric PS I complexes were purified from the wild-type strain of the cyanobacterium *Synechocystis* sp. PCC 6803 using the method of Sun et al. (1998). Optical clarity of the PS I preparations was improved by centrifugation through Spin-X centrifuge filter units (0.2 μm cellulose acetate membrane; Corning Costar, Cambridge, MA). Purity of the PS I preparations was verified by sodium dodecyl sulfate-polyacrylamide gel electrophoresis analysis of the protein subunits. All samples contained 20 mM sodium ascorbate. PS I samples in the dark contain predominantly open reaction centers with unoxidized P700 special pairs (Savikhin et al., 2000).

PS I samples exhibited ~0.3 optical density at the excitation wavelength (660 nm), and were housed in a spinning cell with 0.7-mm pathlength; the excitation density was ~1.5 μJ/cm^2 (1.5 nJ/pulse, ~300-μm spot size). This yielded excitation of one out of every ~1000 Chls. The pump and probe polarizations were separated by 54.7°, to exclude anisotropy effects in the measured kinetics.

RESULTS

Fig. 1 *A* shows the ($P700^+$-P700) difference spectra measured 200 ps (*solid line*) and 3 s (*dashed line*) after exciting the PS I antenna pigments (Savikhin et al., 2001). Both spectra were mutually normalized to the same intensities at wavelengths above 700 nm, where we have observed no time evolution in ΔA after 200 ps. This normalization also leads to the same integrated intensities in both spectra, which is consistent with the fact that excitation and reduction states of Chl *a* molecules that absorb in this spectral region do not change after 200 ps. The difference between 200 ps and 3 s (Fig. 1 *C*, *solid line*) has a characteristic bimodal shape with a negative band at ~691 and a positive band at ~682 nm. Fig. 2 shows time-resolved absorption difference profiles in a 5-μs time window for wild-type PS I. The four probe wavelengths, which span from 680 to 702 nm, bracket the long-time changes in the ($P700^+$-P700) absorption difference spectrum (Fig. 1). At times >1 μs, the signals approach the steady-state ($P700^+$-P700) spectrum. A 300-ns absorption decay component is built upon the asymptotic signal at 690 nm; this is mirrored by a 300-ns absorption rise components at 680 and 685 nm (but not at 702 nm, where the amplitude of the long-time changes in the ($P700^+$-P700) spectrum is very small (Fig. 1 *A*), indicating that the two observed bands in the (3 s − 200 ps) difference spectrum (Fig. 1 *C*) originate from the same process.

At 200 ps, energy transfer as well as charge separation processes in PS I are complete (Hastings et al., 1994; Holzwarth et al., 1993; Brettel and Vos, 1999; Iwaki et al., 1995; Kumazaki et al., 1994; White et al., 1996; Melkozernov, 2001; Savikhin et al., 2001) and the electron is

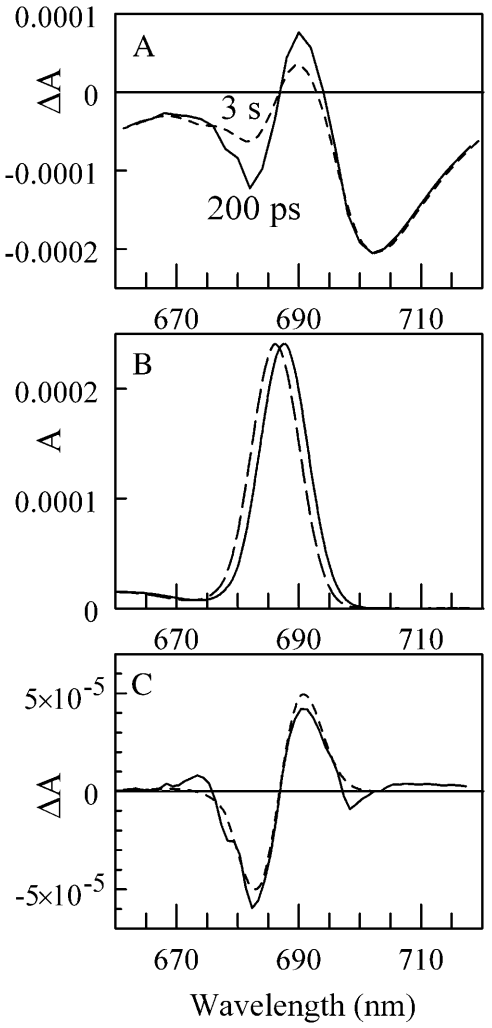

FIGURE 1 (*A*) ($P700^+$-P700) absorption difference spectra measured for wild-type PS I complexes from the cyanobacterium *Synechocystis* sp. PCC 6803 at 200 ps (*solid line*) and 3 s (*dashed line*). (*B*) The single-site A_0 and connecting Chl *a* absorption spectrum in the case when A_1 is reduced (*solid line*) and neutral (*dashed line*) found by fitting ΔA absorption difference spectra shown in Fig. 1 *C* in assumption that only these two Chls experience electrochromic shift. (*C*) The difference between the absorption difference spectra measured at 200 ps and at 3 s (*solid line*), and the difference between two single-site Chl *a* absorption spectra (*dashed line*) shown in plane (*B*).

localized on the secondary acceptor A_1. The consequent electron transfer occurs from A_1 (phylloquinone) to iron sulfur complexes F_X and $F_{A/B}$. None of these cofactors contribute distinctive absorptive bands in the spectral region studied here, and thus cannot be directly responsible for the observed spectral changes. Nevertheless, the measured 300 $\pm$ 50 ns kinetics of the change matches the known ~280-ns electron transfer rate from A_1 to F_X (Bock et al., 1989; van der Est et al., 1994; Brettel, 1988, 1998; Setif and Brettel, 1993; Sakuragi et al., 2002). The second, shorter $A_1 \rightarrow F_X$ electron transfer component has been reported to be $t_{1/2}$ = 6.6 ns (9.5 ns 1/*e* lifetime) in *Synechocystis* sp. (Brettel, 1998)

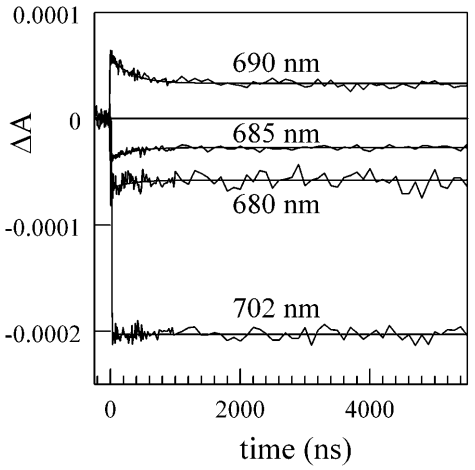

FIGURE 2 Absorption difference profiles in 5-μs window for PS I core antenna/reaction center complexes excited at 660 nm and probed at the indicated wavelengths. Noisy curves are experimental difference profiles; smooth profiles are best fits from global analysis of the four profiles using single-exponential kinetics resulting in optimized lifetime of 300 ns.

and was not observed in our experiment due to the limited time resolution (10–15 ns) and considerable noise level.

The spectral position, amplitude, and bipolar character of the long-time spectral change are consistent with the dynamic shift of a single chlorophyll absorption band (carotenoids do not absorb in the studied spectral region). Such a shift may in principle be introduced by a local protein reorganization that might accompany the electron transfer process, as suggested in Savikhin et al. (2001). Oxidation-induced structural changes were reported, for example, in Kim et al. (2001). Such perturbations in protein structure, however, would not necessarily result in detectable shifts of the Chl absorption band. On the other hand, the transfer of an electron from A_1 to F_X will cause drastic changes in the local electric field that will necessarily lead to an electrochromic shift of the optical transitions of the surrounding Chl *a* pigments. In the following, we will assume that all of the observed nanosecond optical kinetics is caused by an electrochromic shift, and demonstrate that it is consistent with similar effects previously observed in the bacterial reaction center (RC) (Steffen et al., 1994).

The magnitude of the electrochromic shift $\Delta\nu$ of chromophore absorption band depends on the changes in permanent dipole moment $\Delta\vec{\mu}$ and polarizability $\Delta\alpha$ that accompany the optical transition, and the local electric field (Liptay, 1969; Kakitani et al., 1982):

$$\Delta\nu = -\frac{1}{hc}\left(|\Delta\vec{\mu}||\vec{E}_{\text{net}}|\cos\theta + \frac{1}{2}\Delta\alpha E_{\text{net}}^2\right), \qquad (1)$$

where $\vec{E}_{\text{net}}$ is a net electric field at the location of a chromophore due to the presence of an external electric field $\vec{E}$, and θ is the angle between $\Delta\vec{\mu}$ and $\vec{E}_{\text{net}}$; $\Delta\alpha$ is an average scalar polarizability.

The magnitude and direction of the electric field $\vec{E}_e$ at a given atom created by a single electron in vacuum separated by a distance r is given by Coulomb's law:

$$\vec{E}_e = \frac{1}{4\pi\varepsilon_0}\frac{e}{r^2}\hat{r}, \quad (2)$$

where ε_0 is the permittivity of vacuum, e is the charge of an electron, and $\hat{r}$ is the unit vector from this atom to the charge. Within the protein, the electric field of an electron polarizes the nearby amino acids (and other molecules) and the net electric field may be muted (charge screening). The magnitude of this screening depends on the local environment and is defined as the effective static dielectric permittivity (effective dielectric constant) ε_{eff} (Lockhart and Kim, 1992; Steffen et al., 1994):

$$\varepsilon_{eff} = \frac{E_e}{E_{net}}. \quad (3)$$

Because the electric field of an electron is well localized in space (Eq. 2), only the chlorophylls nearest to A_1 will experience significant electrochromic shifts and need to be considered in the first approximation. Although the x-ray structure of PS I from *Synechocystis* sp. has not been determined, its amino acid sequence is highly homologous (especially in the vicinity of the electron transfer chain) to PS I from *Synechococcus elongatus*, whose x-ray structure is known. The main optical differences between the two species relate to the number and energies of the redmost pigments (i.e., pigments absorbing at >705 nm), which do not contribute to the observed signal. According to the x-ray structure of PS I from *Synechococcus elongatus* (Jordan et al., 2001), there are two chlorophylls in the immediate vicinity of A_1: primary electron acceptor A_0 and the ''connecting'' chlorophyll that is believed to facilitate electronic excitation energy transfer from the PS I antenna to the RC (Fig. 3 and Table 1). In the following, we have assumed that electron transfer follows the A-side of the RC. The selection of the active electron transfer branch, however, is not critical for our calculations. Due to the high structural symmetry of the RC, similar estimates of effective dielectric constant (within 10%) can be obtained by assuming that electron transfer occurs along the B-side, or along both sides concurrently.

The direction and magnitude of the electric field $\vec{E}_e$ at the centers of A_0 and the connecting chlorophylls (positions of Mg atoms) was calculated using Eq. 2 assuming that the extra charge on A_1^- is localized in the geometric center of the atoms contributing to the conjugated π system (Table 1).

The magnitude and the absolute direction of the permanent dipole moment change $\Delta\vec{\mu}$ as well as the value of $\Delta\alpha$ of a chromophore molecule can be found by measuring the classical Stark effect—a shift of the absorption band in homogeneous static electric field. Because the effect of the environment on the electric field at the position of the chromophore is not well known, the magnitude of the $|\Delta\vec{\mu}|$ is conventionally measured in units of D/*f*, where *f* is the local field correction factor that relates to the magnitude of the local field $E_{net} = fE_r$ (Boxer, 1993; Böttcher, 1973), and E_r is the average macroscopic electric field in the medium. For monomeric Chl *a* in PS I it has been found that $|\Delta\vec{\mu}| = 0.5\ldots0.8$ (D/*f*) (Rätsep et al., 2000; Zazubovich et al., 2002; Reinot et al., 2001; Frese et al., 2002). A somewhat larger

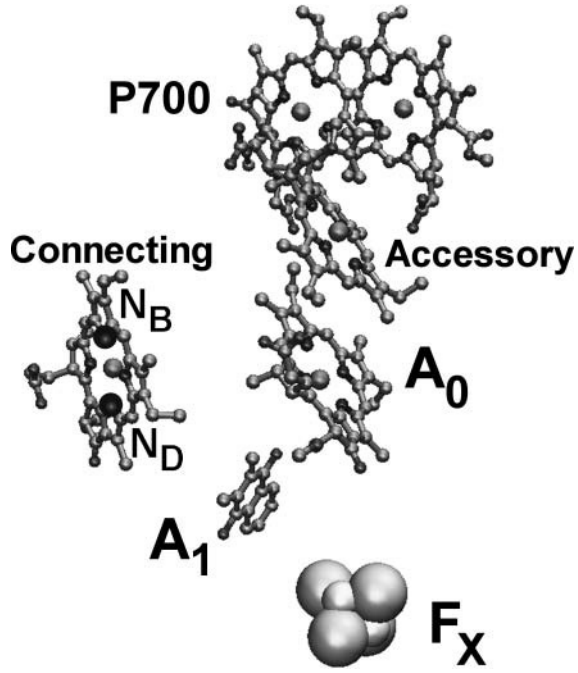

FIGURE 3 The A-branch of the reaction center showing connecting chlorophyll, secondary electron acceptor A_1, and iron-sulfur complex F_X. The positions of N_B and N_D nitrogens are also shown for connecting Chl *a*.

TABLE 1 The parameters used to calculate ε_{eff} based on electrochromic shift of two Chl *a* molecules that are closest to the secondary electron acceptor A_1

	A_0	Connecting
r (Å)	9.0	11.2
E_e (V/m)	1.76×10^9	1.15×10^9
cos(θ)	0.32…0.34	0.47…0.83
$\Delta\nu_e$ (cm^{-1})	−74…−165	−91…−190
$\Delta\nu$ (cm^{-1})	−13	−15
ε_{eff}	6…13	

r, distance from A_1.
E_e, electric field at each of the Chl *a* due to an electron on A_1.
θ , angle between dipole transition moment and electric field vectors.
$\Delta\nu_e$, electrochromic shift expected in absence of screening effect ($\varepsilon_{eff} = 1$).
$\Delta\nu$, an actual shift observed in experiment.
Angle γ was varied between −20° and +20° (see text), $|\Delta\vec{\mu}|$ between 0.5 and 1.0 D/*f*, and $\Delta\alpha$ between 1.5 and 4 $Å^3/f$.

value $|\Delta\vec{\mu}| = 1.02 \pm 0.09$ D/*f* was reported for Chl *a* in a glassy solution (Krawczyk, 1991). In the latter article the value of $\Delta\alpha$ for Chl *a* was also found to vary between 1.5 and 4 $Å^3 f^{-2}$, depending on the number of axial ligands. These values of $|\Delta\vec{\mu}|$ and $\Delta\alpha$ suggest that the observed spectral shift of the absorption band is primarily due to $|\Delta\vec{\mu}|$ (linear term in Eq. 1): even at the highest observed electric fields ($E_e = 1.76 \times 10^9$ V/m, Table 1) and the assumption that $\varepsilon_{eff} = 1$, the quadratic term in Eq. 1, which depends on $\Delta\alpha$, is less than half the size of the linear term.

The local correction factor for chromophores in a protein is typically small: $f = 1.0\ldots1.5$ (Boxer, 1993; Rätsep et al., 2000; Steffen et al., 1994). We will therefore follow Steffen et al. (1994) and use $|\Delta\vec{\mu}|f$ and $\Delta\alpha f^2$ in place of $|\Delta\vec{\mu}|$ and $\Delta\alpha$ when calculating ε_{eff}.

The absolute direction of $\Delta\vec{\mu}$ for Chl *a* (and the similar bacteriochlorophyll *a* molecule) has been determined in Stark effect experiments to be almost colinear with the optical transition moment $\vec{p}$ (Rätsep et al., 1998, Lockhart and Boxer, 1988, Krawczyk, 1991). The largest reported angle γ between these vectors was 20° (Krawczyk, 1991). The transition dipole moment $\vec{p}$ for the Q_y state has been determined to be along the vector connecting N_B and N_D nitrogen atoms (Weiss, 1972; van Zanvoort et al., 1995; Sener et al., 2002). Nitrogens are labeled after Sener et al. (2002) in accordance with the PS I crystallographic data file (Jordan et al., 2001) and are shown in Fig. 3. To obtain negative electrochromic shifts as observed in our experiment, the vector $\Delta\vec{\mu}$ must point in a general direction from N_B to N_D; the opposite direction of $\Delta\vec{\mu}$ (indistinguishable in a conventional Stark effect experiment) would lead to a positive electrochromic shift. This direction of $\Delta\vec{\mu}$ is in agreement with earlier calculations (Eccles and Honig, 1983; Fajer et al., 1992) that predict negative electrochromic shifts when an extra electron is positioned near the N_D side of Chl *a* or similar BChl molecules. To account for possible uncertainty in the angle γ, we varied it within ±20° with respect to the vector connecting N_B and N_D. The angle θ between the electric field $\vec{E}_e$ and $\Delta\vec{\mu}$ was then computed using the known x-ray structure (Jordan et al., 2001). Based on these data, the electrochromic shift $\Delta\nu_e$ for both chlorophylls was calculated under the assumption that there is no electrostatic screening effect from the surrounding molecules (Table 1).

The observed electrochromic shift $\Delta\nu$ is considerably smaller than $\Delta\nu_e$ and indicates significant electrostatic screening of the electron's field. To estimate the magnitude of this screening, we modeled the measured electrochromic difference spectrum (Fig. 1 *C*) using Eqs. 1 and 3 with two electrochromically shifted Chl *a* bands representing A_0 and the connecting pigments, under the assumption that ε_{eff} is the same for both molecules. The Chl *a* single-site absorption spectrum was calculated using the 43 known vibrational frequencies (Gillie et al., 1989; Peterman et al., 1997) with Huang-Rhys factors adjusted to fit the experimental single-site profile at 4 K (Savikhin et al., 2001) (see Fig. 1 *B*). An inhomogeneous Gaussian broadening was applied to this spectrum to yield a bandwidth of 10 nm, a typical bandwidth for Chl *a* in a protein (see, for example, the measured A_0 spectra in Savikhin et al., 2001; Hastings et al., 1994). The amplitude of a Chl *a* absorption band was estimated in the following way: the 3-s ($P700^+$-P700) difference spectrum was modeled as a superposition of four Gaussian components as described in Savikhin et al. (2001). The major 30-nm component centered at 700 nm is conventionally attributed to the bleaching of the low-energy excitonic absorption band of the special pair P700. Because the upper excitonic band of the special pair is not pronounced in the absorption difference spectrum, the oscillator strength of this lower excitonic transition was assumed to be twice that of a single chlorophyll. The intensity of a single Chl *a* band was then adjusted to result in an integrated intensity exactly half of the integrated intensity of the P700 excitonic band. The resulting shape and intensity of the Chl *a* band are in good agreement (within 10%) with the previous direct measurements of the A_0 absorption band (Savikhin et al., 2001; Hastings et al., 1994). Although the spectral position of the A_0 band has been established experimentally to be at ~686 nm (Savikhin et al., 2001; Hastings et al., 1994), the position of the connecting chlorophyll absorption band cannot be determined directly due to considerable spectral congestion (there are almost 100 Chl *a* pigments within PS I antenna absorbing around 680 nm). However, our analysis strongly suggests that the connecting Chl *a* pigment absorption band should be positioned within <5 nm of the A_0 to reproduce the observed spectral features.

Fig. 1 *C* (*dashed line*) shows the result of the fit of the (3 s − 200 ps) difference spectrum under the assumption that both pigments originally absorb at the same wavelength (~686 nm), when $\gamma = 0°$, $\Delta\mu = 0.5$ D/*f* and $\Delta\alpha = 1.5$ $Å^3 f^{-2}$. The best fit was obtained with $\varepsilon_{eff} = 7$, and the corresponding electrochromic shifts for both bands are listed in Table 1. Fig. 1 *B* also shows the net absorption due to these two pigments for the case when A_1 is in neutral (*dashed line*) and reduced (*solid line*) states. Reasonable fits could be obtained only with the assumption that the accessory pigment absorption band lies within <5 nm of the A_0 absorption band. Uncertainties in $\Delta\mu$ (0.5…1.0 D/*f*), $\Delta\alpha$ (1.5…4 $Å^3 f^{-2}$), and γ (−20°…+20°) lead to the range of $\varepsilon_{eff} = 6\ldots13$.

Although the two Chl *a* pigments closest to A_1 experience the largest electrochromic shifts, the rest of the Chl molecules in the PS I complex can also yield significant net electrochromic shift signal, provided that contributions from many pigments add up constructively. Because the actual spectral positions of the pigments is known only for A_0 and P700, precise determination of the electrochromic shift signal due to each pigment is not possible. This may increase the uncertainty in the ε_{eff} value.

To analyze the possible effect on the ε_{eff} value of including the rest of the pigments, we have calculated $\Delta\nu_e$ magnitudes

for all 96 pigments in the PS I structure (Jordan et al., 2001). Each was assumed to have an absorption spectrum similar to the one used for A_0, but the maximum position was allowed to change during the fitting procedure (except for A_0 and P700, whose absorption maximum positions are known). The screening constant ε_{eff} was set to be the same across the PS I interior. Together with ε_{eff}, the number of fitting parameters was 95. These free parameters were then varied to provide the best fit simultaneously to the steady-state absorption spectrum of PS I (not shown) and the electrochromic shift spectrum shown in Fig. 1 *C*. In addition, the parameters were optimized to produce minimal spectral evolution due to the change in the electric field that accompanies electron transfer from F_X to F_A, F_B and out from PS I, as such evolution was not observed in our experiments. The latter constraint turned out to dramatically limit the lowest value of ε_{eff} for which a good fit could be achieved. Perfect fits for all data were obtained with $\varepsilon_{eff} = 6.8$ (Fig. 4 *A*, $\gamma = 0°$, $\Delta\alpha = 1.5$ Å$^3 f^{-2}$, and $\Delta\mu = 0.5$ D/*f*). In this case, the electrochromic shift signal was clearly dominated by the four pigments nearest to A_1: A_0, connecting pigment, and two antenna pigments (ec-A3, A40, A38, and A39 according to the labeling scheme of Jordan et al., 2001). The absorption maxima positions for these four pigments could be varied within ±3 nm of their optimal positions without affecting the quality of the fit. The spectral positions of the rest of the pigments in PS I were not critical; almost any random spectral distribution could be chosen for these pigments (provided that such a distribution results in the observed steady-state absorption spectrum). Uncertainties in $\Delta\mu$ (0.5…1.0 D/*f*), $\Delta\alpha$ (1.5…4 Å$^3 f^{-2}$), and γ (−20°…+20°) lead to the range of $\varepsilon_{eff} = 5…15$.

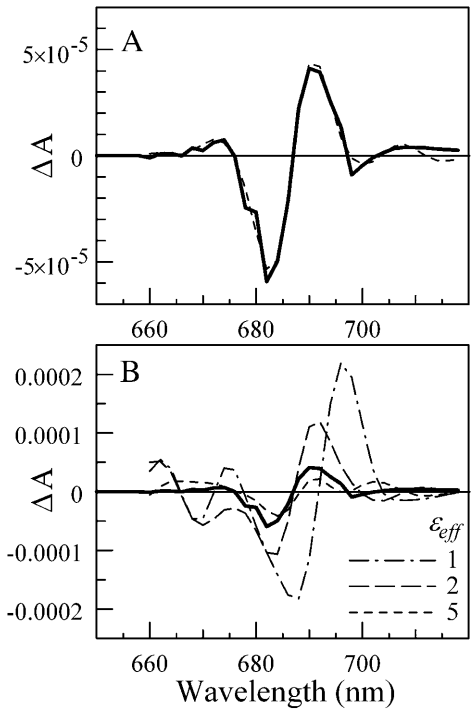

FIGURE 4 (*A*) The measured electrochromic shift signal (*solid line*; the same as in Fig. 1 *C*), and the best fit to the data obtained in a simulation that includes all antenna pigments ($\gamma = 0°$, $\Delta\mu = 0.5$ D/*f*, and $\Delta\alpha = 1.5$ Å^3/*f*). (*B*) Expected electrochromic shift signals in the case of arbitrary spectral distribution of antenna pigments and ε_{eff} fixed at 5 (*short-dashed line*), 2 (*long-dashed line*), and 1 (*dash-dotted line*).

Good fits also could be obtained for ε_{eff} fixed at 3 and 2, but the fitting procedure took considerably longer as progressively more and more pigments had to be arranged in a special manner. If $\varepsilon_{eff} = 3$, both A_0 and the connecting pigment each contribute electrochromic shift signals of comparable magnitude and shape as found in the experiment, and the positions of the next closest pigments must be optimized to lower the overall electrochromic signal. We found that for a good fit, the six closest pigments had to be placed within ±3 nm of their optimal spectral position. When $\varepsilon_{eff} = 2$, each of the four closest to A_1 pigments contributes an electrochromic signal that is larger than or comparable to the total signal observed in the experiment. This fit was sensitive to the position of the 10 closest pigments—the first three pigments had to be within <1 nm of their optimal positions, and the restrictions of the remaining pigments varied progressively from ±2 nm to ±7 nm. Any deviation from the optimal spectral arrangement of these pigments would lead to a drastically different electrochromic shift signal. To illustrate that, Fig. 4 *B* shows the expected electrochromic shift signals for $\varepsilon_{eff} = 1$, 2, and 5 (no fitting, $\gamma = 0°$, $\Delta\mu = 0.5$ D/*f*, and $\Delta\alpha = 1.5$ Å$^3 f^{-2}$) for randomly chosen sets of spectral arrangement of antenna pigments. No fit was possible with $\varepsilon_{eff} \leq 1$.

Good fits were also obtained with ε_{eff} fixed at 8 and 10 ($\gamma = 0°$ and $\Delta\mu = 0.5$ D/*f*); in this case more and more pigments had to be arranged in a special manner so that the net electrochromic shift signal would increase and resemble the experimentally measured signal.

PS I function does not require the optimization of pigment arrangement in a way to produce the observed electrochromic shift spectrum. We find it rather improbable that 10 or more pigments near A_1 happen to be positioned in a such a rare way as to produce the observed electrochromic shift spectrum, as required in the case of $\varepsilon_{eff} = 2$ or 10. Thus, the most probable value for ε_{eff} around A_1 must be in the range $\varepsilon_{eff} = 3…8$. Including uncertainties in $\Delta\mu$ (0.5…1.0 D/*f*), $\Delta\alpha$ (1.5…4 Å$^3 f^{-2}$), and γ (−20°…+20°) would further widen the range of possible values to $\varepsilon_{eff} = 3…20$.

DISCUSSION

The value of the effective dielectric constant ε_{eff} measured in this article is a microscopic parameter and should not be confused with the conventional relative dielectric constant ε_r that characterizes the average macroscopic electric field. There are three main contributors to the ε_{eff} in our case: i), the

presence of a water shell around the protein; ii), the presence of a protein surrounding the chromophore; and iii), the screening of the electric field due to polarization of the chromophore itself.

To estimate the screening effect caused by the water shell, we modeled PS I as an empty spherical cavity within high dielectric constant media ($\varepsilon_r \sim 80$ for water). The size of the cavity and the position of the charge within the cavity were chosen to mimic the size of the PS I complex and the relative position of the secondary electron acceptor A_1. According to this model, the presence of a water shell would lead to a decrease of the electric field (screening) at the position of nearby Chl *a* molecules of the order of 10% or less. Comparably small water shell effects have been reported in Blomberg et al. (1998).

In the case of a medium consisting of similar spherical molecules subjected to a homogeneous external field E_0, the average macroscopic electric field E_r within the medium will be ε_r times smaller than E_0 ($E_r = E_0/\varepsilon_r$), and the local electric field E_{net} in the cavity occupied by one of the molecules can be expressed as $E_{net} = fE_r$, where $f = (\varepsilon_r + 2)/3$ (Böttcher, 1973; Bublitz and Boxer, 1997). Inside a protein ε_r is low (Rosen, 1963; Bone and Pething, 1982, 1985) and values of $f = 1.0\ldots1.5$ are routinely used (Boxer, 1993; Rätsep et al., 2000; Steffen et al., 1994). However, the contribution of the protein medium and the chromophore itself to the value of f is complex in the general case; therefore, in most of the Stark effect studies, the products $f\Delta\mu$ and $f^2\Delta\alpha$ are determined instead. In this article, the latter values were used in place of $\Delta\mu$ and $\Delta\alpha$, respectively, and Eq. 1 should result in a correct prediction of $\Delta\nu$ when $E_r = E_0/\varepsilon_r$ is used in place of E_{net}:

$$\Delta\nu = -\frac{1}{hc}\left(|\Delta\vec{\mu}|\left|f\frac{\vec{E}_0}{\varepsilon_r}\right|\cos\theta + \frac{1}{2}\Delta\alpha\left(f\frac{\vec{E}_0}{\varepsilon_r}\right)^2\right). \quad (4)$$

In the case of an electric field E_e created by an electron on A_1, however, we find that the electrochromic shift is significantly smaller than that predicted by Eq. 4 and expected in a conventional Stark experiment when $E_r = E_e/\varepsilon_r$; instead $E_r = E_e/\varepsilon_{eff}$ must be used with ε_{eff} considerably larger than typical ε_r values for interior of a protein. This discrepancy indicates significant local charge screening, lowering the magnitude of the electric field of an electron in the vicinity of A_1.

Numerous calculations and experiments have shown that the electrostatic properties of proteins depend strongly on the mobility of charged and polar side chains (Pitera et al., 2001; Simonson, 1998; Simonson and Brooks, 1996; Simonson and Perahia, 1995; Rosen, 1963; Bone and Pething, 1982, 1985; Smith et al., 1993). The dielectric constant is a direct measure of the polarizability of the protein medium and reflects its relaxation properties in response to a charge perturbation. The high value of ε_{eff} observed in our experiment suggests that the electron transfer process in PS I is accompanied by a significant reorganization of the surrounding protein structure, leading to effective screening of the electric field produced by the electron. This is consistent with the results obtained in similar experiments on the Stark effect in the bacterial RC (Steffen et al., 1994), where the effective dielectric constant was measured to be $\varepsilon_{eff} \sim 2.5$–$11.6$ at 1.5 K around analogous cofactors constituting the active electron transfer branch. Interestingly, the bacterial reaction center exhibited substantial dielectric asymmetry, with ε_{eff} being 2-5 times smaller along the inactive branch of RC. According to Steffen et al. (1994), the high effective dielectric constant may lead to enhanced electronic coupling between reactant and product states by decreasing the tunneling barrier height and increasing orbital overlap. Our results on PS I support this trend and suggest that a high local dielectric constant is perhaps a common attribute of electron transfer sites in proteins. The effective charge screening and associated reorganizational energy (solvation) may also help to stabilize the product state and prevent back transfer (Treutlein et al., 1992). Due to spectral congestion among the electron transfer cofactors and surrounding pigments, our experiment cannot distinguish between the two almost symmetrical electron transfer branches in PS I.

Recent x-ray structure of PS I (Jordan et al., 2001) reveals 207 water molecules incorporated into this protein structure. Even though the present x-ray resolution is not sufficient to detect all water molecules, it is clear that the concentration of water molecules is especially high in the vicinity of the electron transfer chain formed by secondary electron acceptor A_1 and three iron sulfur complexes F_X, F_A, and F_B. We count a total of 17 water molecules within 7 Å of these cofactors, which leads to ~5 times larger local water concentration in this area than the average water concentration in the rest of the protein. The concentration of water molecules is especially high in the area between A_1 and F_X (Fig. 5). The presence of water around electron transfer cofactors may play a crucial role in increasing structural flexibility of surrounding protein side chains (Bone and Pething, 1985) necessary for achieving effective dielectric screening. The analysis also reveals that polar and charged side chains exhibit significant clustering in the same area.

The proximity of pigments forming the electron transfer chain in PS I to each other and to connecting chlorophylls may cause noticeable excitonic interactions (Witt et al., 2002; Byrdin et al., 2002; Damjanovic et al., 2002). Excitonic interactions are known to lead to an increase in $\Delta\mu$. It has been shown, for example, that the redmost pigments in PS I absorbing at 714 nm exhibit values of $f\Delta\mu = 2.3 \pm 0.20$ D, i.e., about four times larger than monomeric Chl *a* (Rätsep et al., 2000). The latter increase has been attributed to strong excitonic coupling between two or more antenna pigments. The quantitative effect of possible exciton coupling between the pigments surrounding A_1 on values

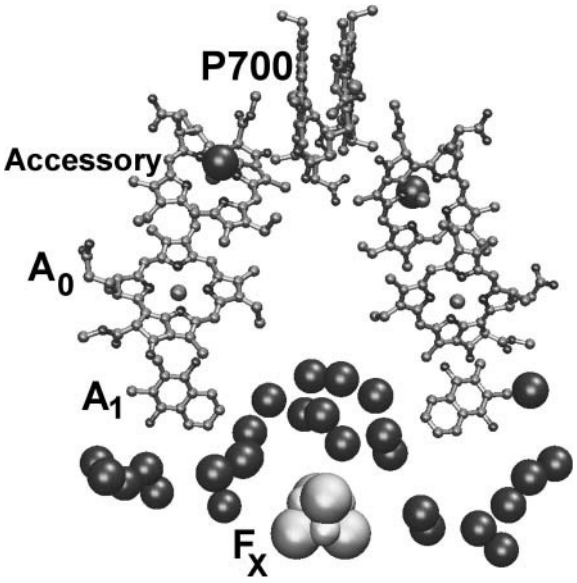

FIGURE 5 The structure of the RC in PS I. Large spheres represent water molecules within 10 Å of the electron transfer chain.

and directions of $\Delta\mu$ is not known. However, the inclusion of this effect into our simulation is expected to increase the electrochromic shift effect (and ε_{eff}), unless the angle θ between $\Delta\vec{\mu}$ and $\vec{E}_{\text{net}}$ for the excitonically coupled molecules would be close to 90° (tentatively 90 ± 10°).

The electric field of an electron positioned on A_1 is well localized in space and thus may serve as a probe of optical properties of the nearby pigments not accessible in conventional optical absorption measurements due to spectral congestion. According to the simulation discussed above, the electrochromic shift of four nearby pigments must account for most of the measured signal. Our recent experiments (to be published) suggest that electron transfer in PS I from *Synechocystis* sp. occurs primarily along the A-branch of the RC, and the four nearest pigments therefore are A_0 (ec-A3), connecting pigment (A40), and two antenna Chls A38 and A39 (Jordan et al., 2001). No visible electrochromic shift signal was observed at wavelengths <675 nm or >700 nm (Fig. 1 *C*), which requires that the absorption maxima of pigments experiencing strong electrochromic shift lie in the range 680–695 nm. The absorption maximum position of A_0 has been measured in independent experiments to be ~686 nm (Savikhin et al., 2001; Hastings et al., 1994), which agrees well with the current conclusion. To the best of our knowledge, optical properties of the other three pigments have not been determined experimentally.

Recently, two groups used the 2.5-Å resolution x-ray structure of PS I from *Synechococcus elongatus* and the available experimental data to calculate Q_y transition energies of all 96 Chl *a* pigments found in PS I (Byrdin et al., 2002; Damjanovic et al., 2002). According to Byrdin et al. (2002), the four pigments nearest to A_1 absorb at wavelengths $\lambda_{\text{ec-A3}} = 683$ nm, $\lambda_{\text{A40}} = 701$ nm, and $\lambda_{\text{A38}} = \lambda_{\text{A39}} = 694$ nm. Strong excitonic coupling between A38 and A39 leads to considerable splitting, resulting in two exciton transitions at 702 and 686 nm with ~85% of the oscillator strength in the upper excitonic band, and is consistent with electrochromic shift data. Somewhat weaker excitonic interaction was calculated for ec-A3 and ec-B2 Chls (labeled as S5 and S3 in Byrdin et al., 2002), and the resulting excitonic bands (674 and 689 nm) would stay close to the optimal positions predicted by our simulations. However, positioning the connecting chlorophyll (A40) at 701 nm would result in a significant negative signal in the region between 700 and 710 nm that was not observed (Fig. 1 *C*).

A different set of transition energies was obtained in Damjanovic et al. (2002) by using the semiempirical INDO/S method and crystal structure of PS I. According to this model, the excitation (diagonal) energies of the four pigments are $\lambda_{\text{ec-A3}} = 685$ nm, $\lambda_{\text{A40}} = 677$ nm, $\lambda_{\text{A38}} = 667$, and $\lambda_{\text{A39}} = 689$ nm. Excitonic interaction between Chls A38 and A39 and mixing with charge transfer states would result in excitonic transitions at ~667 and ~693 nm. Similarly, interaction between ec-A3 and ec-B2 leads to excitonic states absorbing at 676 and 686 nm. The oscillator strength of each of the excitonic bands is not readily available in Damjanovic et al. (2002), and it is possible that the two upper excitonic states (667 and 676 nm) do not contribute effectively to absorption. According to this model, however, the connecting chlorophyll A40 absorbs at 677 nm, which is inconsistent with electrochromic shift data showing negligible signal for wavelengths at and below 677 nm (Fig. 1 *C*).

An intriguing aspect of PS I is the presence of antenna Chl *a* molecules with absorption energies well below that of P700. Among several causes of the red shift, excitonic coupling of two or more Chl *a* molecules has been proposed as the most plausible mechanism (see, for example, Zazubovich et al., 2002; Damjanovic et al., 2002; Byrdin et al., 2002). Based on structural and spectral analysis, Chls A38-A39 were suggested as possible candidates responsible for the extreme red absorption >710 nm (Jordan et al., 2001; Byrdin et al., 2002) in *Synechococcus*. Although it has been shown that the optical properties of the red Chls in *Synechocystis* deviate from those in *Synechococcus* (Zazubovich et al., 2002; Frese et al., 2002), hole-burning studies indicate that the dimers responsible for the redmost absorption in these two species are probably structurally equivalent (Zazubovich et al., 2002). Thus, the absence of electrochromic shift signal at wavelengths >700 nm (Fig. 1 *C*) argues against assigning A38-A39 as redmost Chls. Spectral properties of A38-A39 are of special importance as they are positioned close to the connecting Chl (A40) and may facilitate fast excitation energy transfer from the antenna to P700 (Jordan et al., 2001).

In conclusion, the high effective (local) dielectric constant around electron transfer cofactor A_1 in PS I reported in this work, along with the previously measured high effective dielectric constant along the active electron transfer branch

in bacterial RC (Steffen et al., 1994), indicate that protein reorganization leading to effective charge screening is a necessary structural property of a protein and facilitates effective charge transfer. The electric field of an electron on A_1 also serves as an effective probe of optical properties of nearby pigments, which are not otherwise accessible in conventional absorption experiments due to spectral congestion. The measured electrochromic shift signal implies that the Chls A38 and A39 are not the redmost pigments in PS I. The data presented in this work may serve as an important constraint for improving the accuracy of existing and future models of the energy and electron transfer process in this important protein.

The authors are indebted to Stephen Durbin for useful comments on the manuscript.

This research was supported by the Purdue Research Foundation (grant 6903680). Generation of the PS I complexes was supported by a National Science Foundation grant to P.R.C. (MCB 0078264). Some of the experiments were performed using Ames Laboratory equipment under support from the Division of Chemical Sciences, the Office of Basic Energy Sciences, and the U. S. Department of Energy. Ames Laboratory is operated by Iowa State University under contract W-7405-Eng-82.

REFERENCES

Blomberg, M. R. A., P. E. M. Siegbahn, and G. T. Babcock. 1998. Modeling electron transfer in biochemistry: a quantum chemical study of charge separation in rhodobacter sphaeroides and photosystem II. *J. Am. Chem. Soc.* 120:8812–8824.

Bock, C. H., A. J. van der Est, K. Brettel, and D. Stehlik. 1989. Nanosecond electron transfer kinetics in photosystem I as obtained from transient EPR at room temperature. *FEBS Lett.* 247:91–96.

Bone, S., and R. Pething. 1982. Dielectric studies of the binding of water to lysozyme. *J. Mol. Biol.* 157:571–575.

Bone, S., and R. Pething. 1985. Dielectric studies of protein hydration and hydration-induced flexibility. *J. Mol. Biol.* 181:323–326.

Boxer, S. G. 1993. Photosynthetic reaction center spectroscopy and electron transfer dynamics in applied electric fields. *In* The Photosynthetic Reaction Center. J. Deisenhofer and J. R. Norris, editors. Academic Press, Inc., San Diego, CA. 179–220.

Brettel, K. 1988. Electron transfer from A_1- to an iron-sulfur center with $t_{1/2}$ = 200 ns at room temperature in photosystem I. Characterization by absorption spectroscopy. *FEBS Lett.* 239:93–98.

Brettel, K. 1997. Electron transfer and arrangement of the redox cofactors in photosystem I. *Biochim. Biophys. Acta.* 1318:322–373.

Brettel, K., and M. H. Vos. 1999. Spectroscopic resolution of the picosecond reduction kinetics of the secondary electron acceptor A_1 in photosystem I. *FEBS Lett.* 447:315–317.

Brettel, K. S. 1998. Electron transfer from acceptor A_1 to the iron-sulfur cluster in photosystem I measured with a time resolution of 2 ns. *In* Photosynthesis: Mechanisms and Effects. G. Garab, editor. Kluwer Academic Publishers, Dordrecht, The Netherlands. 611–614.

Bublitz, G. U., and S. G. Boxer. 1997. Stark spectroscopy: applications in chemistry, biology and materials science. *Annu. Rev. Phys. Chem.* 48: 213–242.

Byrdin, M., P. Jordan, N. Krauss, P. Fromme, D. Stehlik, and E. Schlodder. 2002. Light harvesting in photosystem I: modeling based on the 2.5-Å structure of photosystem I from *Synechococcus elongatus*. *Biophys. J.* 83:433–457.

Böttcher, C. J. F. 1973. Theory of Dielectric Polarization. Elsevier, Amsterdam, The Netherlands.

Damjanovic, A., H. M. Vaswani, P. Fromme, and G. R. Fleming. 2002. Chlorophyll excitations in photosystem I of *Synechococcus elongatus*. *J. Phys. Chem. B.* 106:10251–10262.

Eccles, J., and B. Honig. 1983. Charged amino acids as spectroscopic determinants for chlorophyll *in vivo*. *Proc. Natl. Acad. Sci. USA.* 80: 4959–4962.

Fajer, J., L. K. Hanson, M. C. Zerner, and M. A. Thompson. 1992. Suggestions for directed engineering of reaction centers: metal, substituent and charge modifications. *In* The Photosynthetic Bacterial Reaction Center II. J. Brenton and A. Vermeglio, editors. Plenum Press, New York. 33–42.

Frese, R. N., M. A. Palacios, A. Azzizi, I. H. M. van Stokkum, J. Kruip, M. Rönger, N. V. Karapetyan, E. Schlodder, R. van Grondelle, and J. P. Dekker. 2002. Electric field effects on red chlorophylls, betta-carotenes and P700 in cyanobacterial photosystem I complexes. *Biochim. Biophys. Acta.* 1554:180–191.

Gillie, J. K., G. J. Small, and J. H. Golbeck. 1989. Nonphotochemical hole burning of the native antenna complex of photosystem I (PSI-200). *J. Phys. Chem.* 93:1620–1627.

Hastings, G., F. A. Kleinherenbrink, S. Lin, T. J. McHugh, and R. E. Blankenship. 1994. Observation of the reduction and reoxidation of the primary electron acceptor in photosystem I. *Biochemistry.* 33:3193–3200.

Holzwarth, A. R., G. Schatz, H. Brock, and E. Bittersmann. 1993. Energy transfer and charge separation kinetics in photosystem I. Part 1: Picosecond transient absorption and fluorescence study of cyanobacterial photosystem I particles. *Biophys. J.* 64:1813–1826.

Iwaki, M., S. Kumazaki, K. Yoshihara, T. Erabi, and S. Itoh. 1995. Photosynthesis. M. Mathis, editor. Kluwer, Dordrecht, The Netherlands. 147–150.

Jordan, P., P. Fromme, H. T. Witt, O. Klukas, W. Saenger, and N. Krauss. 2001. Three-dimensional structure of cyanobacterial photosystem I at 2.5 Å resolution. *Nature.* 411:909–917.

Kakitani, T., B. Honig, and A. R. Crofts. 1982. Theoretical studies of the electrochromic response of carotenoids in photosynthetic membranes. *Biophys. J.* 39:57–63.

Kim, S., C. A. Sacksteder, K. A. Buixby, and B. A. Barry. 2001. A reaction induced FT-IR study of cyanobacterial photosystem I. *Biochemistry.* 40:15384–15395.

King, G., F. S. Lee, and A. Warshel. 1991. Microscopic simulations of macroscopic dielectric constants of solvated proteins. *J. Chem. Phys.* 95:4366–4377.

Klukas, O., W. D. Schubert, P. Jordan, N. Krauss, P. Fromme, H. T. Witt, and W. Saenger. 1999. Photosystem I, an improved model of the stromal subunits PsaC, PsaD, and PsaE. *J. Biol. Chem.* 274:7351–7360.

Krauss, N., W. Hinrichs, I. Witt, P. Fromme, W. Pritzkow, Z. Dauter, C. Betzel, K. S. Wilson, H. T. Witt, and W. Saenger. 1993. Three-dimensional structure of system I of photosynthesis at 6 Å resolution. *Nature.* 361:326–331.

Krauss, N., W. D. Schubert, O. Klukas, P. Fromme, H. T. Witt, and W. Saenger. 1996. Photosystem I at 4 A resolution represents the first structural model of a joint photosynthetic reaction centre and core antenna system. *Nat. Struct. Biol.* 3:965–973.

Krawczyk, S. 1991. Electrochromism of chlorophyll a monomer and special pair dimer. *Biochim. Biophys. Acta.* 1056:64–70.

Kumazaki, S., M. Iwaki, I. Ikegami, H. Kandori, K. Yoshihara, and S. Itoh. 1994. Rates of primary electron transfer reactions in the photosystem I reaction center reconstituted with different quinones as the secondary acceptor. *J. Phys. Chem.* 98:11220–11225.

Liptay, W. 1969. Electrochromism and solvatochromism. *Angew. Chem. Internat. Edit.* 8:177–188.

Lockhart, D. J., and S. G. Boxer. 1988. Stark effect spectroscopy of *Rhodobacter sphaeroides* and *Rhodopseudomonas viridis* reaction centers. *Proc. Natl. Acad. Sci. USA.* 85:107–111.

Lockhart, D. J., and P. S. Kim. 1992. Internal Stark effect measurement of the electric field at the amino terminus of an α helix. *Science*. 257: 947–951.

Löffler, G., H. Schreiber, and O. Steinhauser. 1997. Calculation of the dielectric properties of a protein and its solvent: theory and a case study. *J. Mol. Biol.* 270:520–534.

Melkozernov, A. N. 2001. Excitation energy transfer in photosystem I from oxygenic organisms. *Photosynth. Res.* 70:129–153.

Moser, C. C., J. M. Keske, K. Warncke, S. F. Farid, and P. L. Dutton. 1992. Nature of biological electron transfer. *Nature*. 355:796–802.

Peterman, E. J. G., T. Pullerits, R. van Grondelle, and H. van Amerongen. 1997. Electron-phonon coupling and vibronic fine structure of light-harvesting complex II of green plants: temperature dependent absorption and high-resolution fluorescence spectroscopy. *J. Phys. Chem. B*. 101: 4448–4457.

Pierce, D. W., and S. G. Boxer. 1992. Dielectric relaxation in a protein matrix. *J. Phys. Chem.* 96:5560–5566.

Pitera, J. W., M. Falta, and W. F. van Gunsteren. 2001. Dielectric properties of proteins from simulations: the effect of solvent, ligands, pH, and temperature. *Biophys. J.* 80:2546–2555.

Reinot, T., V. Zazubovich, J. M. Hayes, and G. J. Small. 2001. New insights on persistent nonphotochemical hole burning and its application to photosynthetic complexes. *J. Phys. Chem. B*. 105:5083–5098.

Rosen, D. 1963. Dielectric properties of protein powders with adsorbed water. *Trans. Faraday. Soc.* 59:2178–2191.

Russell, A. J., and A. R. Fersht. 1987. Rational modification of enzyme catalysis by engineering surface charge. *Nature*. 328:496–500.

Rätsep, M., T. W. Johnson, P. R. Chitnis, and G. J. Small. 2000. The red-absorbing chlorophyll *a* antenna states of photosystem I: a hole-burning study of *Synechocystis* sp. PCC 6803 and its mutants. *J. Phys. Chem. B*. 104:836–847.

Rätsep, M., H.-M. Wu, J. M. Hayes, R. E. Blankenship, R. J. Cogdell, and G. J. Small. 1998. Stark hole-burning studies of three photosynthetic complexes. *J. Phys. Chem.* 102:4035–4044.

Sakuragi, Y., B. Zybailov, G. Shen, A. D. Jones, P. R. Chitnis, A. van der Est, R. Bittl, S. Zech, D. Stehlik, J. H. Golbeck, and D. A. Bryant. 2002. Insertional inactivation of the menG gene, encoding 2-phytyl-1,4-naphthoquinone methyltransferase of Synechocystis sp. PCC 6803, results in the incorporation of 2-phytyl-1,4-naphthoquinone into the A1 site and alteration of the equilibrium constant between A_1 and F_X in Photosystem I. *Biochemistry*. 41:394–405.

Savikhin, S., W. Xu, P. R. Chitnis, and W. S. Struve. 2000. Ultrafast primary processes in PS I from Synechocystis sp. PCC 6803: roles of P700 and A_0. *Biophys. J.* 79:1573–1586.

Savikhin, S., W. Xu, P. Martinsson, P. R. Chitnis, and W. S. Struve. 2001. Kinetics of charge separation and $A_0^- \rightarrow A_1$ electron transfer in photosystem I reaction centers. *Biochemistry*. 40:9282–9290.

Schnier, P. D., D. S. Gross, and E. R. Williams. 1995. Electrostatic forces and dielectric polarizability of multiply protonated gas-phase cytochrome *c* ions probed by ion/molecule chemistry. *J. Am. Chem. Soc.* 117:6747–6757.

Sener, M. K., D. Lu, T. Ritz, S. Park, P. Fomme, and K. Schulten. 2002. Robustness and optimality of light harvesting in cyanobacterial photosystem I. *J. Phys. Chem. B*. 106:7948–7960.

Setif, P., and K. Brettel. 1993. Forward electron transfer from phylloquinone A_1 to iron-sulfur centers in spinach photosystem I. *Biochemistry*. 32:7846–7854.

Simonson, T. 1998. Dielectric constant of cytochrome *c* from simulations in a water droplet including all electrostatic interactions. *J. Am. Chem. Soc.* 120:4875–4876.

Simonson, T., and C. L. Brooks, III. 1996. Charge screening and the dielectric constant of proteins: insights from molecular dynamics. *J. Am. Chem. Soc.* 118:8452–8458.

Simonson, T., and D. Perahia. 1995. Internal and interfacial dielectric properties of cytochrome *c* from molecular dynamics in aqueous solution. *Proc. Natl. Acad. Sci. USA*. 92:1082–1086.

Smith, P. E., R. M. Brunne, A. E. Mark, and W. F. van Gunsteren. 1993. Dielectric properties of trypsin inhibitor and lysozyme calculated from molecular dynamics simulations. *J. Phys. Chem.* 97:2009–2014.

Steffen, M. A., K. Lao, and S. G. Boxer. 1994. Dielectric asymmetry in the photosynthetic reaction center. *Science*. 264:810–816.

Sun, J., A. Ke, P. Jin, V. P. Chitnis, and P. R. Chitnis. 1998. Isolation and functional study of photosystem I subunits in the cyanobacterium *Synechocystis* sp. PCC 6803. *Methods Enzymol.* 297:124–139.

Treutlein, H., K. Schulten, A. T. Brünger, M. Karplus, J. Deisenhofer, and H. Michel. 1992. Chromophore-protein interactions and the function of the photosynthetic reaction center: a molecular dynamics study. *Proc. Natl. Acad. Sci. USA*. 89:75–79.

van der Est, A., C. Bock, J. Golbeck, K. Brettel, P. Setif, and D. Stehlik. 1994. Electron transfer from the acceptor A_1 to the iron-sulfur centers in photosystem I as studied by transient EPR spectroscopy. *Biochemistry*. 33:11789–11797.

van Zanvoort, M. A. M. J., D. Wróbel, P. Lettinga, G. van Ginkel, and Y. K. Levine. 1995. The orientation of the transition dipole moments of chlorophyll *a* and pheophytin *a* in their molecular frame. *Photochem. Photobiol.* 62:299–308.

Varadarajan, R., T. E. Zewert, H. B. Gray, and S. G. Boxer. 1989. Effects of buried ionizable amino acids on the reduction potential of recombinant myoglobin. *Science*. 243:69–72.

Weiss, C. J. 1972. The pi electron structure and absorption spectra of chlorophylls in solution. *J. Mol. Spectrosc.* 44:37–80.

White, N. T. H., G. S. Beddard, R. G. Thorne, T. M. Feehan, T. E. Keyes, and P. Heathcote. 1996. Primary charge separation and energy transfer in the photosystem I reaction center of higher plants. *J. Phys. Chem.* 100:12086–12099.

Witt, H., E. Schlodder, C. Teutloff, J. Niklas, E. Bordignon, D. Carbonera, S. Kohler, A. Labahn, and W. Lubitz. 2002. Hydrogen bonding to P700: site-directed mutagenesis of threonine A739 of photosystem I in *Chlamidomonas reinhardtii*. *Biochemistry*. 41:8557–8569.

Woodbury, N., and J. P. Allen. 1995. The pathway, kinetics and thermodynamics of electron transfer in wild type and mutant reaction centers of purple nonsulfur bacteria. *In* Anoxygenic Photosynthetic Bacteria. R. E. Blankenship, M. T. Madigan, and C. E. Bauer, editors. Kluwer, Dordrecht, The Netherlands. 527–557.

Zazubovich, V., S. Matsuzaki, T. W. Johnson, J. M. Hayes, P. R. Chitnis, and G. J. Small. 2002. Red antenna states of photosystem I from cyanobacterium *Synechococcus elongatus*: a spectral hole burning study. *Chem. Phys.* 275:47–59.

Zinth, W., and W. Kaiser. 1993. Time-resolved spectroscopy of the primary electron transfer in reaction centers of *Rhodobacter sphaeroides* and *Rhodopseudomonas viridis*. *In* The Photosynthetic Reaction Center. J. Deisenhofer and J. Norris, editors. Academic Press, London, UK. 71.